JOURNAL OF VIROLOGY, Aug. 1976, p. 579-593
Vol. 19, No. 2

Printed in U.S.A.

Defective Bud Formation in Human Cells Chronically Infected with Subacute Sclerosing Panencephalitis Virus

M. DUBOIS-DALCQ,* T. S. REESE, M. MURPHY, AND D. FUCCILLO

Infectious Diseases Branch and Laboratory of Neuropathology and Neuroanatomical Sciences, National Institute of Neurological and Communicative Disorders and Stroke, Bethesda, Maryland 20014

Received for publication 20 January 1976

Human prostate cells chronically infected with the Mantooth strain of subacute sclerosing panencephalitis (SSPE) virus multiply normally, fuse only occasionally to form giant cells, and yet have twisted intracytoplasmic nucleocapsids. These cells are able to support replication of vesicular stomatitis virus, although they release only small amounts of SSPE virus. To determine why carrier cells do not produce virus, they were examined with techniques for surface replication, freeze-fracturing, and immunoperoxidase labeling with SSPE antibody. The surface of carrier cells, like that of productive cells, is characterized by ridges crowned with viral antigens and devoid of the intramembrane particles revealed by freeze-fracture techniques. Since surface ridges form where nucleocapsids attach to the membrane, the shape and length of ridges are indicative of the shape and length of the underlying nucleocapsid. Whereas ridges on productive cells are serpentine in shape, those on carrier cells are typically straight or hairpin shaped, and the hairpin ridges are twice as long as serpentine ridges on productive cells. Furthermore, the spacing between ridges on carrier cells is never as small as that in productive infections, so that continuous sheets of viral membrane are never formed. The majority of carrier cells lack the round viral buds observed in productive cells but have, instead, many elongated processes attached to the cell surface. Each of these processes contains one or two hairpin ridges overlying hairpin-shaped nucleocapsids. These "hairpin buds" are restricted to a single region of the carrier cell surface, whereas viral buds are distributed over the entire surface of productive cells. Thus, there are several structural defects in carrier cells that depend on the specific interaction of a certain viral strain with a certain cell type. These defects prevent the deployment of viral antigen in some regions of the cell surface, the formation of nucleocapsids of normal length, the coiling of attached nucleocapsids, and the consolidation of sheets of viral membrane into spherical buds with the nucleocapsids coiled inside. These defects may account for the failure of carrier cells to shed infectious virus.

Cultured cells can be chronically infected with measles virus and therefore constitute a tool to study the mechanism of chronic measles infection (11, 12, 22, 25-27, 30, 35, 36). By selection of a less destructive virus, or of cells resistant to lysis by the virus, chronically infected measles carrier cells have been obtained without the use of antibody (27). These carrier cells show almost no cytopathic effects and produce a small amount, if any, of infectious virus. While they contain intracytoplasmic viral antigen as well as nucleocapsids embedded in a granular coat (21, 25), the amount and distribution of membrane antigens vary in different cell lines. In some, no viral antigens are found on the plasma membrane (25), whereas in others a polar distribution has been observed (11). However, no alignment of nucleocapsids or budding of virus has been detected (21, 25).

Similar carrier cell lines chronically infected with subacute sclerosing panencephalitis (SSPE) strains of measles virus were described recently (3, 5). These cell lines were derived by co-cultivating indicator cells with cells from brains of SSPE patients. One of these carrier cell lines is characterized by numerous smooth nucleocapsids and the absence of nucleocapsid alignment and viral bud formation on giant cells (7). However, another type of carrier state, characterized by a paucity in giant cells, can be induced by direct infection of cultured cells with an SSPE strain (37). This carrier cell line was chosen for our study because a high percentage of the cells carried viral antigens (37).

The application of freeze-fracturing and surface replication techniques combined with immunolabeling methods has demonstrated extensive changes in membrane structure during viral development in productive infection with SSPE virus (9). In the present study, we compare the biological properties and structure of one SSPE carrier cell line with those of cells productively infected with measles and SSPE viruses to identify the defects that prevent the production of infectious virus in carrier cells.

MATERIALS AND METHODS

Virus and cells. Cells from a continuous cell line derived from a human prostate adenoma (MA 160 cells) were infected with the Mantooth strain of SSPE virus to produce a carrier cell line. The Mantooth virus was isolated by co-cultivating brain cells in primary cultures with HeLa cells (17). Free virus isolated from these co-cultures was used after one more passage in HeLa cells. A carrier cell line designated MA 72046 was established with these viruses in MA 160 cells by M. M. Vincent (Microbiological Associates, Inc., Bethesda, Md.) by the method of Rustigian (35). For the ultrastructural study, cells from passages 25 to 30 of the carrier cell line (MA 72046) were usually studied, but later passages, as well as uninfected cells (MA 160), were sampled also. For studies with thin sectioning or freeze-fracturing, cells were treated with trypsin and seeded into large Falcon plastic flasks. Monolayers of cells were also grown in 35-mm plastic petri dishes containing 12-mm glass cover slips in preparation for surface replication and immunolabeling experiments. In some instances, 1 volume of trypsin-treated carrier cells was co-cultivated with 1 or 2 volumes of Vero cells (Flow Laboratories, Inc., Rockville, Md.) and observed for the occurrence of cytopathic effect (17). The growth medium for all experiments consisted of Eagle minimum essential medium supplemented with 10% heat-inactivated fetal calf serum and 100 U of penicillin G and 100 μg of streptomycin sulfate per ml. Cultures were incubated in a 37°C incubator with 5% CO_2.

For comparative studies, productive infection with four strains of virus was produced in Vero cells. Viruses were gathered from the fifth passage of measles virus Edmonston B strain, the third passage of SSPE virus Mantooth strain (17), the fourth passage of SSPE virus Halle strain (9, 15), and the third passage of SSPE virus McClellan strain (6), all in Vero cells. The SSPE Halle virus was plaque purified and also studied in MA 160 cells. In all experiments with measles or SSPE viruses, multiplicity of infection varied between 0.01 and 1. The Indiana strain of vesicular stomatitis virus (VSV) was obtained from Robert Lazzarini and inoculated into carrier cells at a multiplicity of infection of 10. Titrations of VSV were done in baby hamster kidney (BHK-21) cells, and plaques were counted at 18 h (4).

Test for virus production and measles antigenicity. Free virus and cell-associated virus were assayed by the PFU test on Vero cells grown in a medium containing methylcellulose (4). Hemadsorption was performed with rhesus monkey erythrocytes (24). Indirect fluorescent-antibody staining was performed on cells fixed in methanol for the detection of intracellular antigen (15) and on living cells for the detection of membrane antigen (20). Indirect immunoperoxidase (IP) labeling was performed after glutaraldehyde fixation for the detection of surface antigen as described previously (6, 7). Briefly, various dilutions of SSPE serum with high measles antibody titers were first applied to the cells for 1 h. Monolayers were then rinsed, and goat anti-human immunoglobulin G coupled to peroxidase (Miles Laboratories, Rehovoth, Israel) was added at a globulin concentration of 0.05 mg/ml. After 1 h, cells were washed overnight, postfixed in glutaraldehyde, and incubated in a peroxide-diaminobenzidine substrate (6). As a control for specificity, infected cells were treated similarly with human serum with no measles antibodies detectable by the hemagglutination inhibition and fluorescent-antibody tests.

Electron microscopy. Viral particles and intracellular nucleocapsids were examined after negative staining. For free virus, supernatant fluids were collected from 3- to 7-day-old cultures, whereas for cytoplasmic nucleocapsids the cells were disrupted by osmotic shock. After clarification, both free virus and nucleocapsids were concentrated at 37,000 $\times$ g for 30 min at 4°C (18). Sediments were suspended in a small amount of culture medium, stained with 2% potassium phosphotungstate (pH 6.8), and layered on Formvar-coated grids.

For surface replication (2, 9), cells grown on glass cover slips were fixed in 1% glutaraldehyde in 0.1 M cacodylate buffer for 30 min, rinsed, and postfixed in 1% osmium tetroxide in the same buffer for 1 h. Osmium fixation was omitted in immunolabeling experiments. After fixation, cells were dehydrated quickly and air dried, or, in a few instances, the critical point drying method was used instead (1). Cover slips with dried cells were placed on top of the specimen stage of a Balzer 360 M freeze-etch apparatus, and a replica was made at 105°C by using an electron beam gun for platinum shadowing.

For freeze-fracturing, fixation was performed with the aldehyde fixative described previously (9). Cells were then scraped out of the flasks, centrifuged at 3,000 rpm, rinsed with buffer, progressively equilibrated with 25% glycerol in water, frozen in Freon 22, and stored in liquid nitrogen prior to being fractured in the freeze-etch apparatus at −118°C. All replicas were cleaned in methanol and Chlorox before being mounted on Formvar-coated grids.

For thin sectioning, pellets as well as monolayers of immunolabeled cells were postfixed in osmium tetroxide, stained with uranyl acetate at pH 5, dehydrated in graded alcohols, and embedded in Epon. Electron micrographs were taken on a Philips 201 electron microscope. Some carrier cells were serially sectioned and mounted on Formvar-coated slot grids.

Structures seen in surface replicas and negatively stained preparations were measured with a Hewlett-Packard Digitizer. Student's t test was used for the statistical analysis.

RESULTS

Biological properties. Table 1 compares the properties of the SSPE Mantooth virus-infected carrier cells with those of Vero cells productively infected with the Halle strain of SSPE virus. Productive infections of cells with other SSPE and measles strains were also studied, but their properties were quite similar to the Halle infection. Therefore, the properties of Halle virus infection given in Table 1 are representative of productive infection with other strains of measles virus. The carrier cells showed few cytopathic changes even 7 days after transfer, whereas 3 days after inoculation with the Halle strain most of the Vero cells were lysed and detached from the substrate. A small proportion of carrier cells had 5 to 10 nuclei, whereas giant cells in the productive infection had hundreds of nuclei and covered two-thirds of the monolayer even after 2 days. Fusion and lysis were also characteristic of MA 160 cells infected with SSPE Halle strain and of Vero cells infected with SSPE Mantooth and McClellan strains as well as the Edmonston B strain of measles virus. However, in these instances, the infection took 2 or 3 days longer to spread over the entire monolayer. The amount of hemadsorption was identical in both carrier and productive cells. In productive infections, the number of Vero cells with intracytoplasmic viral antigen detected by fluorescent antibody increased from 50% on day 2 to 100% on day 3 after viral inoculation, whereas in the chronic infection 80 to 90% of the cells contained viral antigen 2 days after a passage, when the cells were still in the growth phase. Cytoplasmic inclusions of viral antigen were often found in carrier cells undergoing mitosis. Membrane antigen, as detected by fluorescent antibody or IP staining, was present in both chronic and productive infection but was evenly distributed in cells productively infected with the SSPE Halle strain and present only at the poles of most of the carrier cells (11).

Plaque assays of carrier cultures revealed less than 50 infectious particles per ml of the supernatant fluid. Freezing and thawing carrier cells from the same passage liberated as many as 10^5 PFU/ml into the medium. In contrast, the supernatant fluids of cultured Vero cell monolayers infected with SSPE Mantooth, Halle, and McClellan viruses and measles Edmonston B viruses had titers of 6×10^5, 1×10^7, 1.4×10^5, and 5×10^6 PFU/ml, respectively. The titers of cell-associated virus were 3 to 4 logarithmic units lower than those of the cell-free virus. Infectious particles obtained from the carrier cultures produced smaller plaques that formed after longer incubation periods than with control viruses.

In other experiments, monolayers of carrier cells were superinfected with measles Edmonston B, SSPE Halle, or SSPE Mantooth virus. Cytopathic changes in the carrier cells were evident in all instances. Infectious particles at titers as high as 6×10^4 PFU/ml were detected in the supernatant fluid at 72 h after superinfection with all viruses except SSPE Mantooth. However, our titrations did not allow distinction between the newly assembled superinfecting virus and infectious particles from the Mantooth virus already in the carrier cells. VSV also reproduced well in carrier cell monolayers, resulting in 1.6×10^9 PFU/ml of supernatant, but the normal 12- to 14-h lytic cycle was extended to more than 30 h.

Subcellular structure. The sequence of membrane changes in carrier cells differed greatly from those in productive SSPE virus infection (6, 7, 9, 15, 33, 34). In productive infections in MA 160 or Vero cells infected with SSPE Halle strain, as well as in Vero cells infected with SSPE Mantooth strain or the measles Edmonston B strain, the surface of the giant cells was covered with twisted ridges seen in surface replicas (Fig. 1). These were oriented in various directions and assumed sinuous shapes, like an S, or a U shape (Fig. 1). Ridges were seen in areas in which the virus-modified membrane protruded over a nucleocapsid lying under the plasmalemma (Fig. 2, arrows) (9).

TABLE 1. *Properties of productive and carrier cell lines*

Cells	Cytopathic effect	Frequency of cell fusion	Hemadsorption	Cells with viral antigen (%)	Distribution of viral antigen	Infective particles (PFU/ml)		Appearance of plaques
						Cell free[a]	Cell associated[b]	
Productive[c]	+++	+++	++	100	Diffuse	10^7	10^3	Early and large
Carrier[d]	−	+	++	80–90	Polar	0–100	10^5	Late and various sizes

[a] Supernatant.
[b] Freeze-thawed.
[c] Halle strain in Vero.
[d] Mantooth strain in human prostate cells.

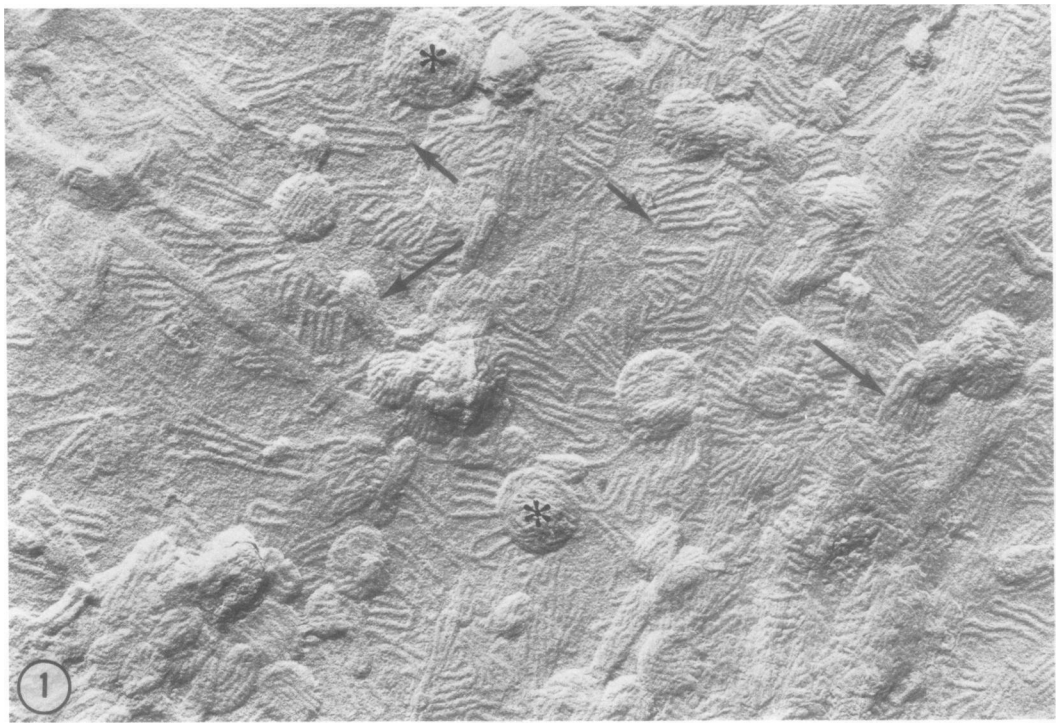

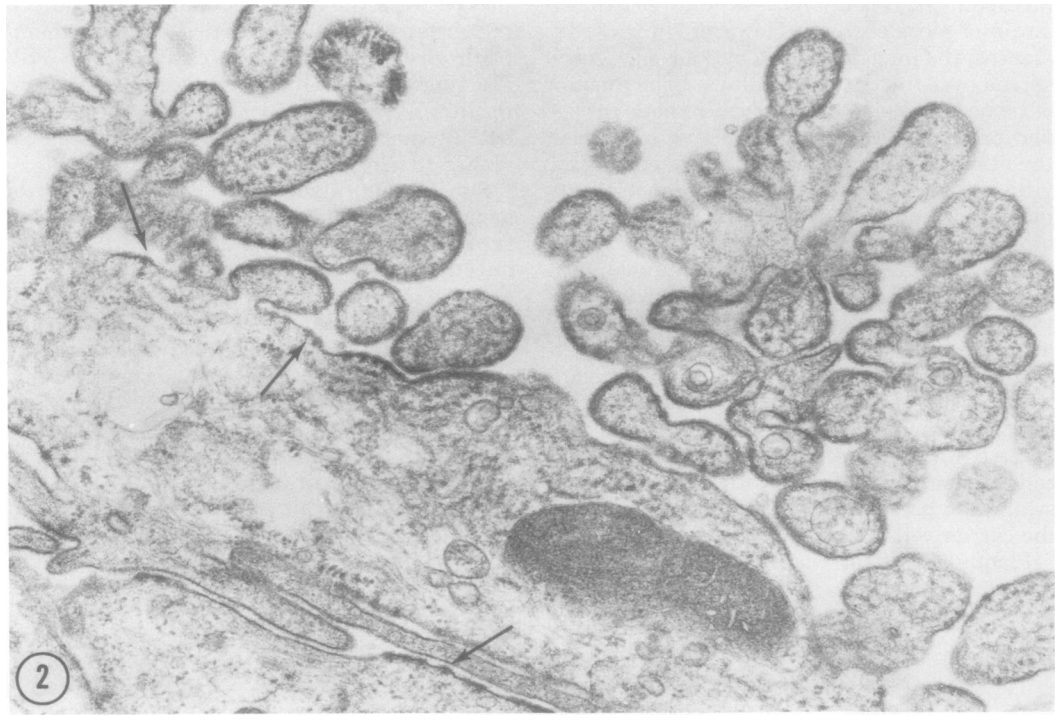

FIG. 1. *Surface replica of a human prostate cell (MA 160) acutely infected with the Halle strain of SSPE virus. Much of the surface of this giant cell is covered with twisted ridges and viral buds (asterisks). The ridges have a random orientation and assume various shapes such as an S or O, or a U (short arrows). Most of the viral buds are spherical and covered with ridges, which are more closely apposed to each other than on the adjacent membrane. A few buds are club shaped (long arrows).* ×18,000.

FIG. 2. *Thin section of a Vero cell acutely infected with the Halle strain of SSPE virus. Groups of viral buds and viruses cluster near the surface of a cell containing nucleocapsids. Ridges are scattered over the cell surface (arrows). The limiting membrane of the round buds has an increased density due to the presence of a continuous coat of surface projections and of an internal fuzz around the nucleocapsids. Nucleocapsids are not seen clearly at this magnification.* ×25,000.

Twisted ridges were also present on the viral buds, and the spacing between them was less than in the surrounding cell membrane (Fig. 1) (9). Most of the viral buds were spherical although some were club shaped (Fig. 1, long arrows). That these structures were indeed viral buds is illustrated in Fig. 2, which shows viral buds and particles containing nucleocapsids in a thin section through a cell at a stage of viral production identical to that shown in Fig. 1. The membrane surrounding viral buds or covering nucleocapsids at ridges was characterized by projections on its outer surface and a fuzzy material on the inner surface of the membrane. Groups of nucleocapsids were also seen in the cytoplasma (Fig. 2).

Ninety percent of the carrier cells, when examined in thin sections (Fig. 3), typically contained cytoplasmic viral inclusions similar to those found in productive cells. However, no nuclear inclusions of the type seen in late stages of productive infection (15, 33, 34) were found. The cytoplasmic inclusions consisted of twisted tubules surrounded by a fuzzy coat. Since cytoplasmic nucleocapsids isolated from these cells displayed the typical herringbone structure of pseudomyxovirus nucleocapsids (Fig. 3, left inset) (31), these tubules were assumed to be nucleocapsids. The isolated nucleocapsids were measured and compared with those obtained from productive cells; no significant differences in length were found. Since nucleocapsids are frequently fragmented during concentration (Fig. 3) (13, 39), comparative measurements of their lengths are open to question.

Carrier cells usually differ from productive cells by the presence of elongated processes forming groups at one pole of the cell (Fig. 3). Examination of these processes in serial sections showed that they are usually branched and are extensions of the carrier cell plasma membrane. Unlike the normal microvilli, the plasma membrane limiting those processes had an increased density (Fig. 3) similar to that observed on round viral buds on productive cells. With higher magnification, it was apparent that the characteristic membrane density was mainly due to surface projections (Fig. 3, right inset; see Fig. 14). Details of the internal structure of these processes are given below.

In surface replicas, ridges were found on most carrier cells but only in certain well-delineated regions of the cell surface (Fig. 4, left). The rest of the surface was devoid of any structural changes and was similar to that of uninfected cells (Fig. 4, right). The ridges on the majority of carrier cells, in contrast to those on productive cells (Fig. 1), were straight, usually parallel with adjacent ridges, and widely spaced (Fig. 4). Some formed rigid hairpins of various lengths, sometimes as long as 5 μm (Fig. 4, arrows; Fig. 6). Thin sections through adjacent pairs of ridges, presumably forming the arms of hairpins, showed that the plasma membrane was covered with surface projections and protruded over both nucleocapsids (see Fig. 12, inset). Fuzzy, dense material extended between the nucleocapsids and the inner surface of the plasma membrane. Since viral nucleocapsids always lie under plasma membrane ridges, a close correspondence in shape and length must exist between surface ridges and nucleocapsids. Surface replicas allow surveys of large areas of cell surfaces, so that the running length of many ridges on the cell surfaces could be measured (Fig. 8). The lengths of straight and hairpin ridges on carrier cells were compared to the twisted ridges on the productive cells. The majority of the twisted ridges were approximately 1 μm long, a value similar to that of the longest measles virus nucleocapsids measured after purification (38). The distribution of ridge lengths in the carrier cells was more spread out, with small peaks at 2, 4, and 5 μm. Also, the mean length of carrier cell ridges was twice that of ridges in productive infection, and this difference was highly significant. For reasons given above, these differences in the shapes and lengths of ridges probably reflect differences in the shape and length of the underlying nucleocapsids, at least of those parts interacting with the plasma membrane.

Surface replicas showed that carrier cells with straight ridges also had numerous elongated processes that differed strikingly from the microvilli seen in control cells (Fig. 5). These processes were usually dried into a mat on the surface in air-dried specimens and appeared to correspond to the elongated processes with thickened membranes identified in thin sections (Fig. 3). Like the ridges, these processes were confined to one pole of the carrier cell surface. The detailed structure of these processes was examined more easily and illustrated better in regions where they were more sparse. One or two long hairpin ridges were found in each of these processes (Fig. 7, short arrows). These ridges appeared to be longer than the twisted ridges on the round buds of productive cells (cf. Fig. 1 and 5), but it was not possible to obtain reliable measurements of ridges on productive cells because their whole lengths could not be followed on the curved surface of the spherical viral buds. The long processes in the carrier cells were always attached to the cell surface but, unlike the budding processes in productive cells (Fig. 16 in

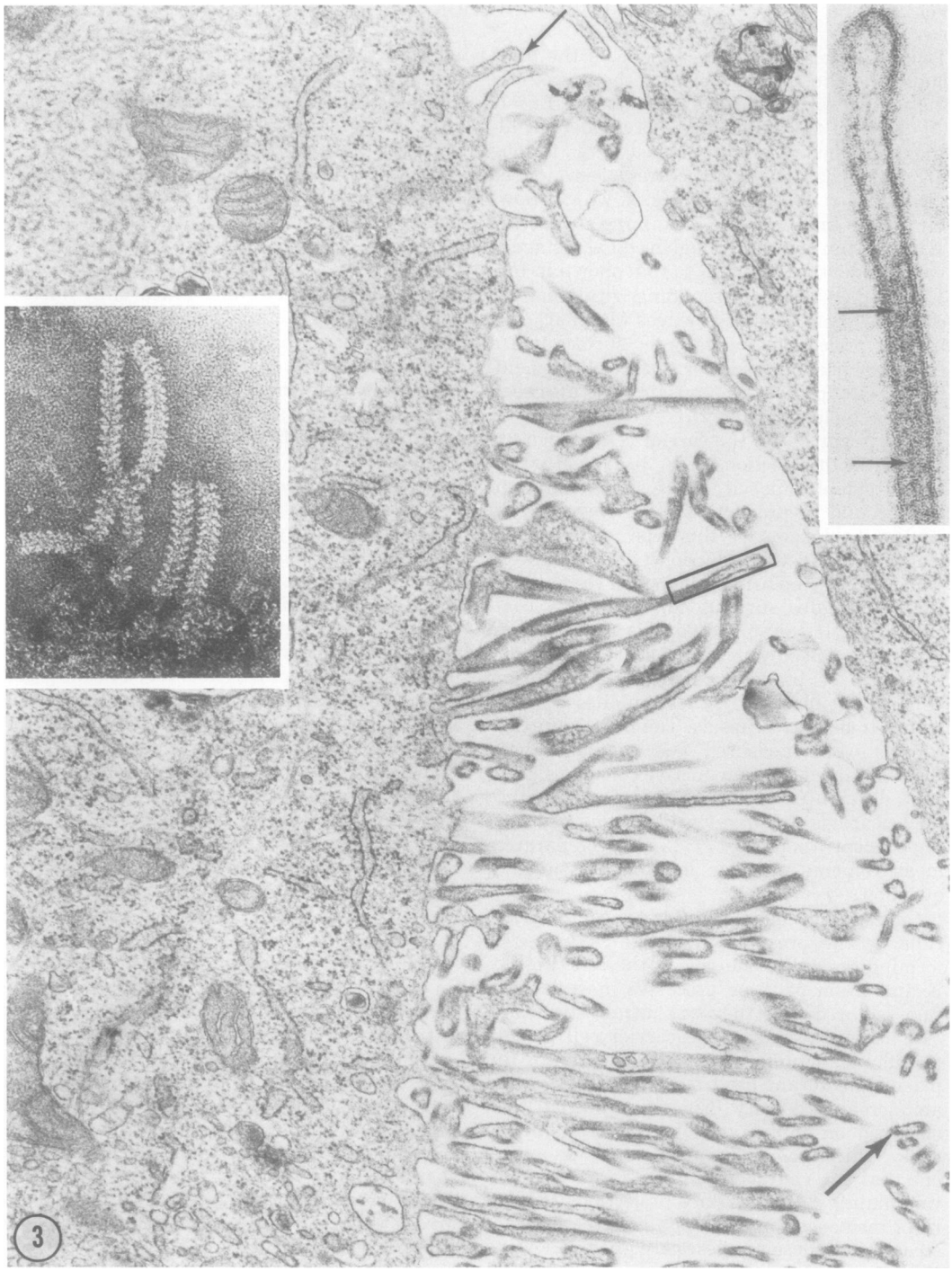

FIG. 3. *Thin sections through a carrier cell (MA 72046). A cytoplasmic inclusion of twisted viral tubules occupies the upper left corner. These nucleocapsids, when concentrated and negatively stained, show the herringbone structure typical of pseudomyxovirus nucleocapsids, but they are frequently broken (left inset). A few microvilli (short arrow) are seen in the upper part of the picture, whereas numerous elongated processes originate from other regions of the same cell. These processes are sometimes branched or transversally cut (large arrow), and their membranes look thicker than the normal cell membrane. A portion of one of these processes, framed in the center of the picture, is enlarged in the right inset. This process is covered with a continuous coat of surface projections, and a portion of one internal tubule can be detected (arrows; see Fig. 14). ×30,000; left inset, ×217,000; right inset, ×140,000.*

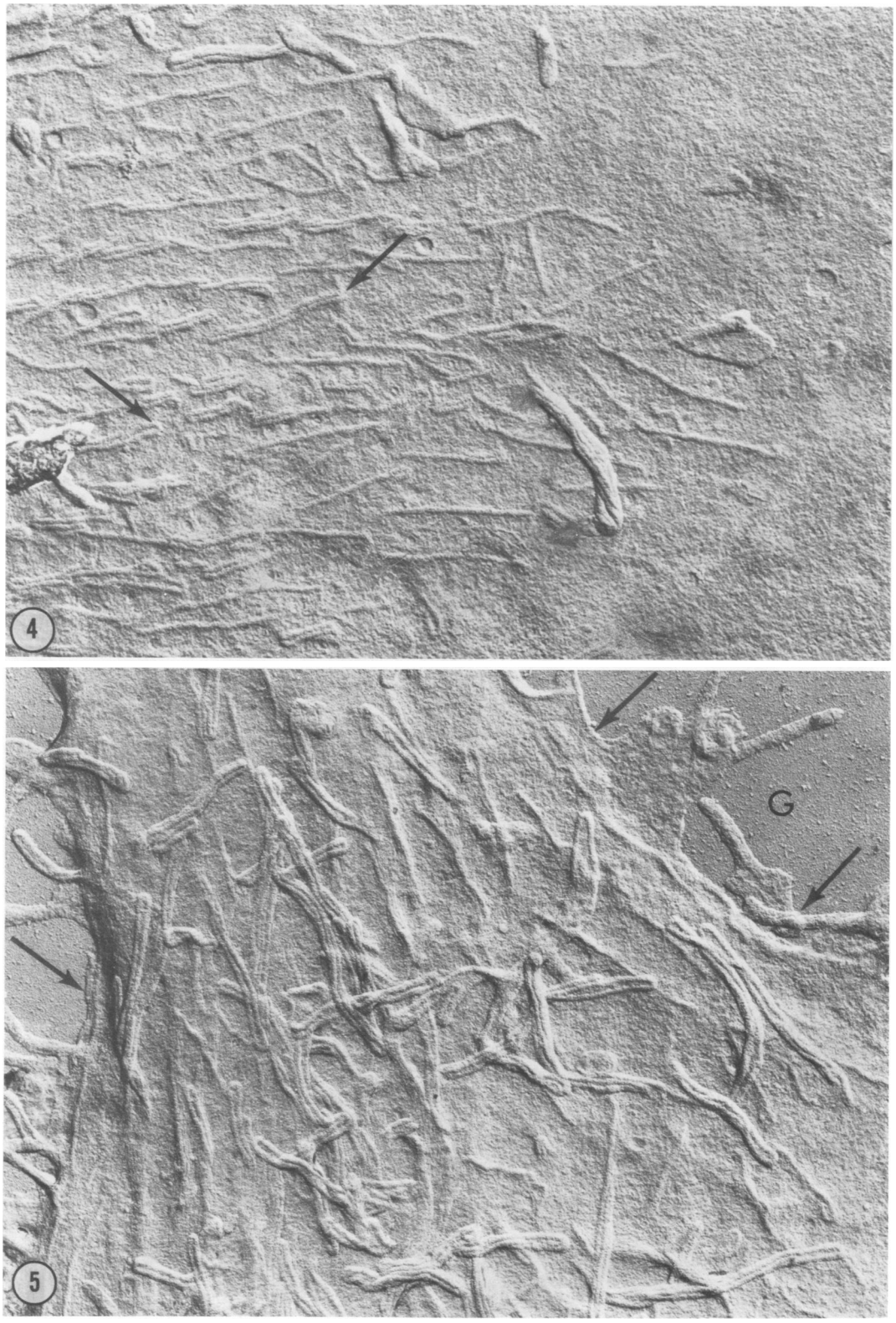

FIG. 4. *Surface replica of a carrier cell. Some regions of the cell surface are devoid of structural changes (at the right), whereas numerous widely spaced ridges are present in other regions (at the left). Most of these ridges are straight, although a few (arrows) form tight hairpins.* ×18,000.

FIG. 5. *In addition to the straight ridges scattered over its surface, this carrier cell bears numerous elongated processes, many of which are matted together, probably as a result of flattening onto the cell surface during drying. Most of these processes are covered with two or more hairpin ridges. Arrows point to edges of the cell. G indicates glass surface.* ×18,000.

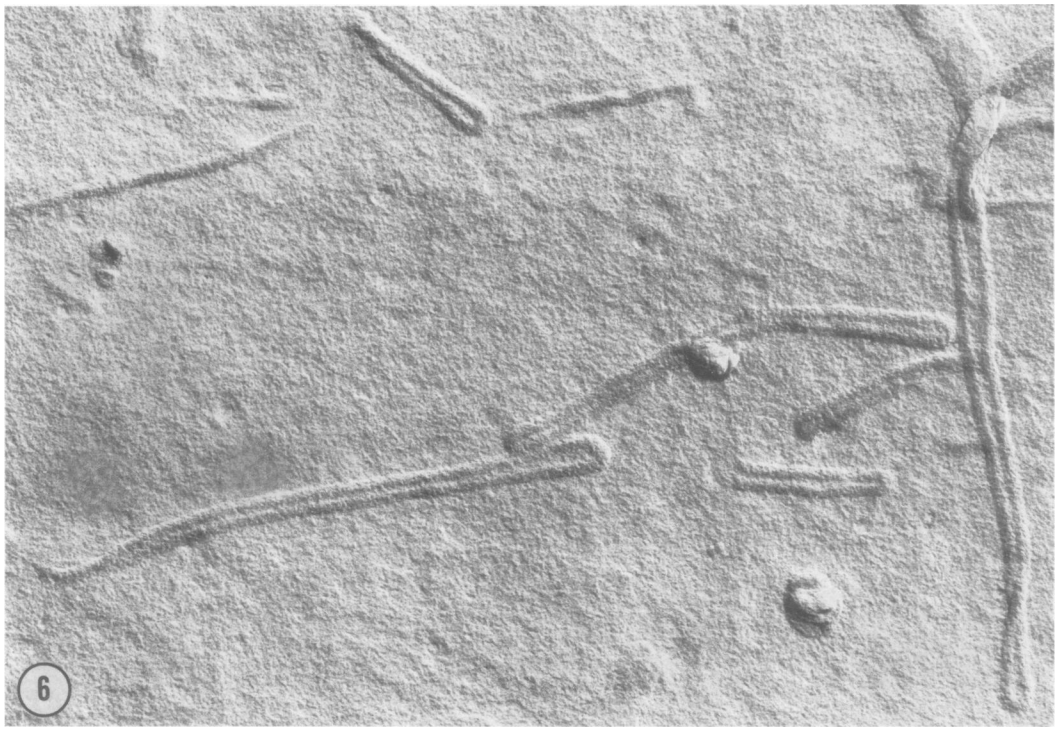

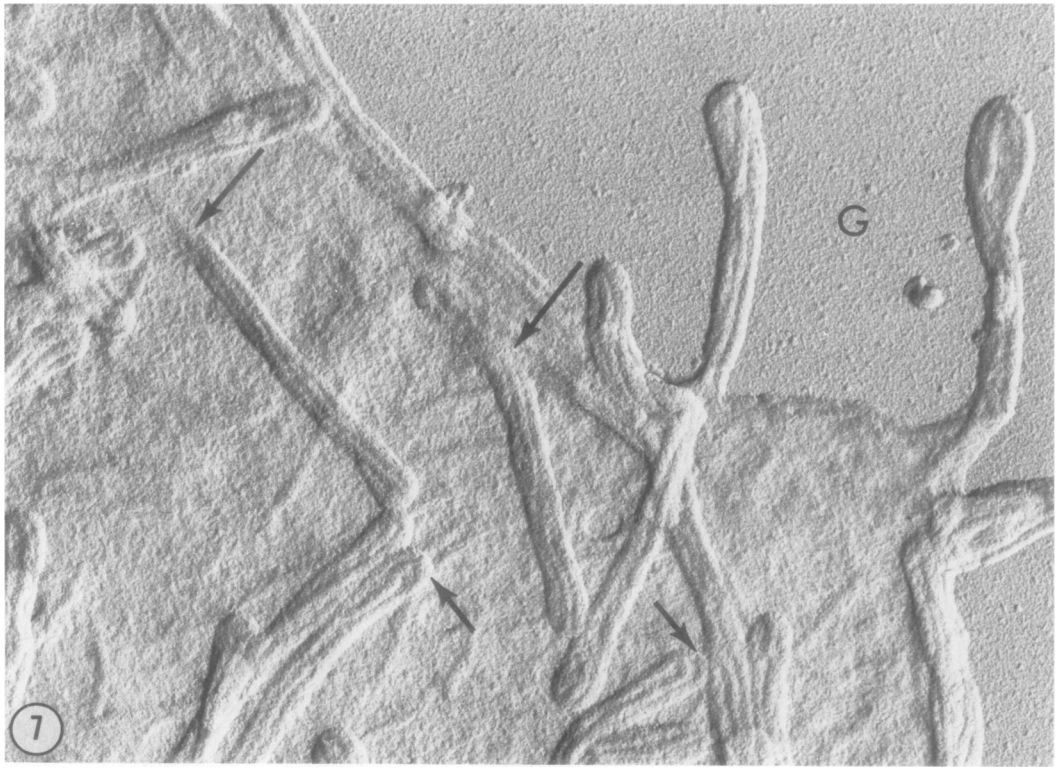

FIG. 6. *Several of the hairpin type of ridges are scattered over a portion of the surface of a carrier cell surface. The longest hairpins are approximately four times as long as the shortest ones.* ×32,000.

FIG. 7. *Inside each elongated process in this carrier cell are two intertwined hairpin ridges. The short arrows indicate the tips of elongated processes where the separate hairpin ridges are seen clearly. Unlike viral buds in productively infected cells, the point of attachment of these processes to the cell surface is not narrower than the rest of the process (long arrows). G indicates glass surface.* ×31,000.

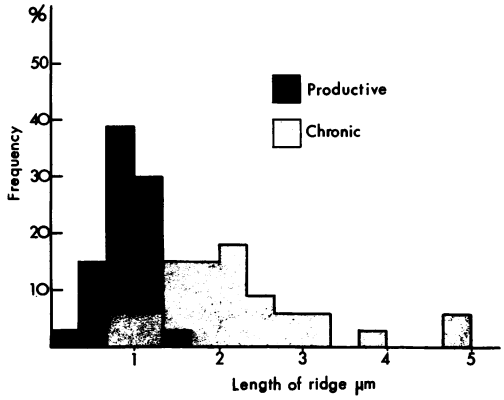

FIG. 8. *Frequency of the lengths of ridges measured on pictures of surface replicas of productive (black blocks) and carrier cells (clear blocks). Comparative measurements were made of twisted ridges (productive infection) adjacent to viral buds and rigid hairpin ridges (chronic infection). These measurements of ridges reflect the distribution of lengths of the nucleocapsids in contact with the plasmalemma since these nucleocapsids are always covered by ridges. In productive cells, a sharp peak of ridge length is found at 1 µm, whereas in carrier cells the length distribution is more spread out, with a major peak at 2 µm and smaller ones at multiples of 1 µm.*

reference 9), the necks of these processes were not narrower than the process itself (Fig. 7 and 9, long arrows).

In surface replicas of carrier cells dried by the critical point method, a fine particulate material, which was not detectable after air drying, appeared on the crests of ridges (Fig. 9). Some ridges on the cell membrane were in continuity with hairpin ridges on elongated processes (Fig. 9, arrows). The processes were usually covered with packed granular subunits, which distinguished them from microvilli attached to uninfected cells since villi had few granular particles on their surface (Fig. 10). Indirect IP labeling with SSPE serum, followed by air drying and surface replication, was used to determine whether the packed granular subunits on ridges were associated with the viral antigens on the surface of carrier cells. Hairpin ridges were indeed covered with granules of label (Fig. 12), and patches of label were also present outside of the ridges, although most regions of the carrier cell surfaces were devoid of label. The labeling was thought to be specific for viral antigens since carrier cells treated with negative serum did not have granules of label on the ridges or the adjacent membrane and their surfaces looked like unlabeled cells (Fig. 11).

Freeze-fractured ridges in carrier cells were characterized by their paucity of intramembrane particles (Fig. 13), and the finely granular appearance of the fractured surfaces was similar to that observed on the twisted ridges of productive cells (9). The number, shape, and distribution of ridges inside the membrane of freeze-fractured carrier cells were similar to those of the ridges seen in surface replicas.

Longitudinal sections cut through elongated processes, occasionally passed in the plane of a hairpin-shaped nucleocapsid lying under the membrane. These had the 5-nm transverse periodicity typical of pseudomyxovirus nucleocapsids (Fig. 14). The more frequent cross sections through elongated processes revealed the presence of two or four nucleocapsids under the modified membrane, probably corresponding to one or two hairpin nucleocapsids (Fig. 14, right inset). Three or five viral tubules were occasionally found in cross sections of the elongated processes. This suggested that, in addition to one or two hairpin nucleocapsids, one straight viral tubule was also present or that the arms of some hairpins were of unequal lengths. The spacing between nucleocapsids inside of the elongated processes was approximtely 70 nm and did not differ from the smallest spacing detected between nucleocapsids under the adjacent membrane (insets, Fig. 12 and 14). This lack of difference in spacing contrasts with the large difference in spacing characteristic of productive cells, where membrane-associated nucleocapsids were separated by 67 nm and those in buds by 46 nm (9).

In surface replicas, elongated processes were heavily labeled by the indirect IP method, and this labeling was also apparent in thin sections (Fig. 14). On the same cell surface, microvilli adjacent to these labeled elongated processes were devoid of specific label (Fig. 14, left inset), although both types of surface projections were equally accessible to the antibody.

Groups of elongated processes could be recognized in freeze-fracture replicas (Fig. 15) since they had a typical polar distribution not observed with microvilli of control cells. They were similar in shape to the elongated processes illustrated in Fig. 3. Their diameter could vary along their length, and some of them were branched. Where fine details could be resolved, ridges were identified on the inner half of the membrane covering these processes, and these had characteristics similar to those of the ridges seen on the adjacent membrane (compare Fig. 16 with Fig. 13). Depending on the plane of fracture, ridges were seen entering processes at their base (Fig. 16) or traveling along their side (Fig. 17).

Because of their similar distribution on the cell surface, their branched, elongated shapes, and the presence of ridges and nucleocapsids

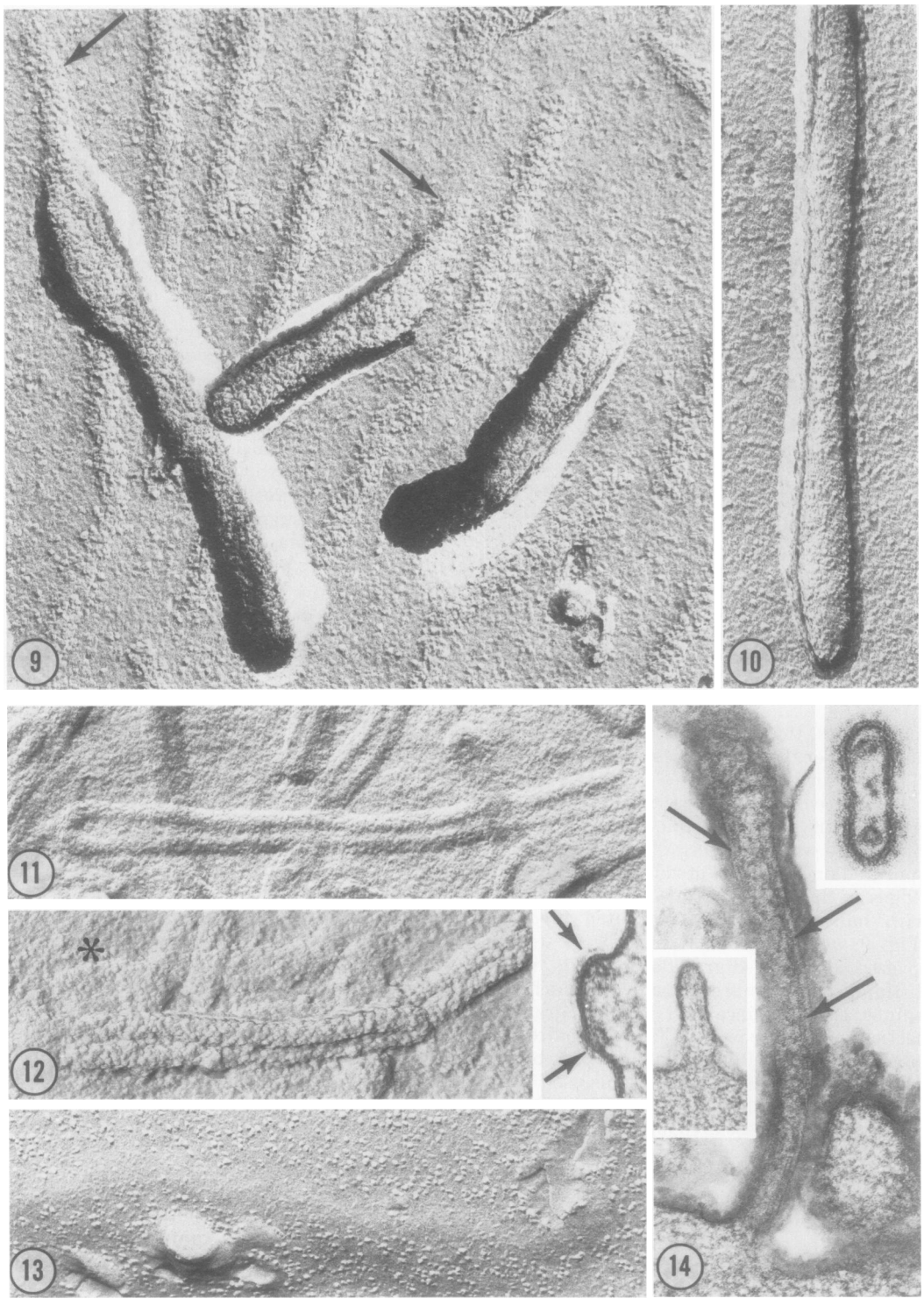

FIG. 9. *In carrier cells prepared by the critical point drying method, granular subunits are packed at the crests of ridges and on adjacent elongated processes. A few granules are scattered on the rest of the cell surface. Points where ridges on the surrounding cell surface are reflected onto the surface of the elongated processes at their attachment with the plasmalemma are indicated by arrows.* ×68,000.

FIG. 10. *Microvillus from an uninfected cell that was critical point dried. Normal microvilli are characterized by scattered granules similar to those on the rest of the surface of uninfected cells. There is no aggregation of granular subunits like those on elongated processes of carrier cells (Fig. 9).* ×68,000.

along their length, we concluded that the elongated processes seen in surface replicas, in thin sections, and with the freeze-fracture technique represent different aspects of a single population of viral-induced processes. Small discrepancies in their apparent shapes and sizes with different techniques are presumed to be due to several factors. First, the dehydration and embedding for thin sectioning or the dehydration for surface replication would produce considerable shrinkage, which should not occur during preparation for freeze-fracturing. This could account for the elongated processes looking larger and more rounded in the freeze-fracture replica than with the other techniques. Conversely, processes passing out of the plane of freeze-fracture have rounded tips, which might be mistaken for true ends of these processes; this effect should make these processes look shorter after freeze-fracturing than in surface replicas.

In passages 25 to 29 of the carrier cells, a large majority of the cells, approximately 80%, had rigid hairpin ridges and elongated processes, whereas two other cell types, representing 10 to 20% of the cell population, showed a different deployment of ridges. One type consisted of cells with no structural changes or viral antigen on their surface. The other type of cell had the twisted ridges and round buds characteristic of productive infections. The numbers of these two types of cell fluctuated from one passage to another. Indeed, after passage 30, cells with twisted ridges and round buds increased in number and were mixed with the cells bearing hairpin ridges. Some cells had both round buds and elongated processes with ridges. These changes might reflect a morphological transition from the carrier to the productive type of infection, but this was not substantiated by a significant increase in the titer of free virus. When Vero cells were added to carrier cells at these passages, fusion to form giant cells occurred within 2 days (16) although Vero cells had no effect on earlier passages.

DISCUSSION

The biological properties of our carrier cell line are very similar to those of regulated or carrier infections established with other measles virus strains (11, 22, 26, 27, 30, 35) as well as to the properties of the IP-3-Ca subline of SSPE virus (3). However, none of these previously described carrier cells contains as much cell-associated virus as do the carrier cells selected for the present study. Furthermore, superinfection with other SSPE or measles strains, as well as with VSV, results in the release of a substantial amount of virus. When VSV is inoculated into carrier cells, typical bullet-shaped buds are recognized on carrier cells, indicating that VSV can replicate in these cells (unpublished data). Similar experiments with strains of measles virus showed that the resistance of carrier cells to superinfection is limited to the SSPE strain originally used to create the chronic infection. Therefore, the arrest of maturation appears to be specific for the Mantooth SSPE strain.

By comparing surface replicas with thin sections and combining these approaches with immunolabeling methods, it has been possible to identify structural changes in the plasma membrane of carrier cells, which differ strikingly from those in productively infected cells (9). Carrier cells typically have straight and hairpin ridges on their surfaces instead of the twisted ones that characterize productive cells. Furthermore, hairpin ridges are twice as long as the twisted ridges on productive cells. However, these membrane ridges have several features in common with those on productive cells. The membrane surface in both is crowned by granular subunits, which are the sites of viral antigens, and both are formed where a nucleocapsid contacts a region of the plasma membrane lacking intramembrane particles. Hairpin ridges are also characteristic of the elongated processes clustered at one pole of carrier cells. The ridges, as well as the size, shape, and

FIG. 11 and 12. *Details of hairpin ridges in carrier cells air dried without (Fig. 11) or with (Fig. 12) immunoperoxidase labeling with SSPE serum. In Fig. 12, granules of label 15 to 25 nm in diameter are tightly packed along the hairpin ridges, whereas in Fig. 11 the hairpin ridge is smooth and bears no granules. The membrane adjacent to the labeled hairpin has only small patches of diffuse reaction product (asterisk). Inset shows a cross section through an unlabeled ridge. Two viral tubules are present under the membrane, each crowned by surface projections (arrows). ×45,000; inset, ×140,000.*

FIG. 13. *Freeze-fractured membrane from carrier cell, showing a straight ridge. Along the ridge, the membrane is devoid of the particles typical of the rest of the membrane. ×60,000.*

FIG. 14. *Thin section splitting a long process from an immunolabeled carrier cell. The surface of the process is strongly labeled, and long viral tubules (arrows), possibly arms of a single hairpin, lie just under the membrane. This heavy label is specific on certain regions of the membrane since a microvillus from the same immunolabeled cell has almost no label (left inset). The right inset shows a cross section through an unlabeled elongated process containing two nucleocapsids that are probably different arms of a hairpin nucleocapsid. Fuzzy projections from the membrane surface are gathered on the membrane over the underlying nucleocapsids. ×72,000; left inset, ×45,000; right inset, ×180,000.*

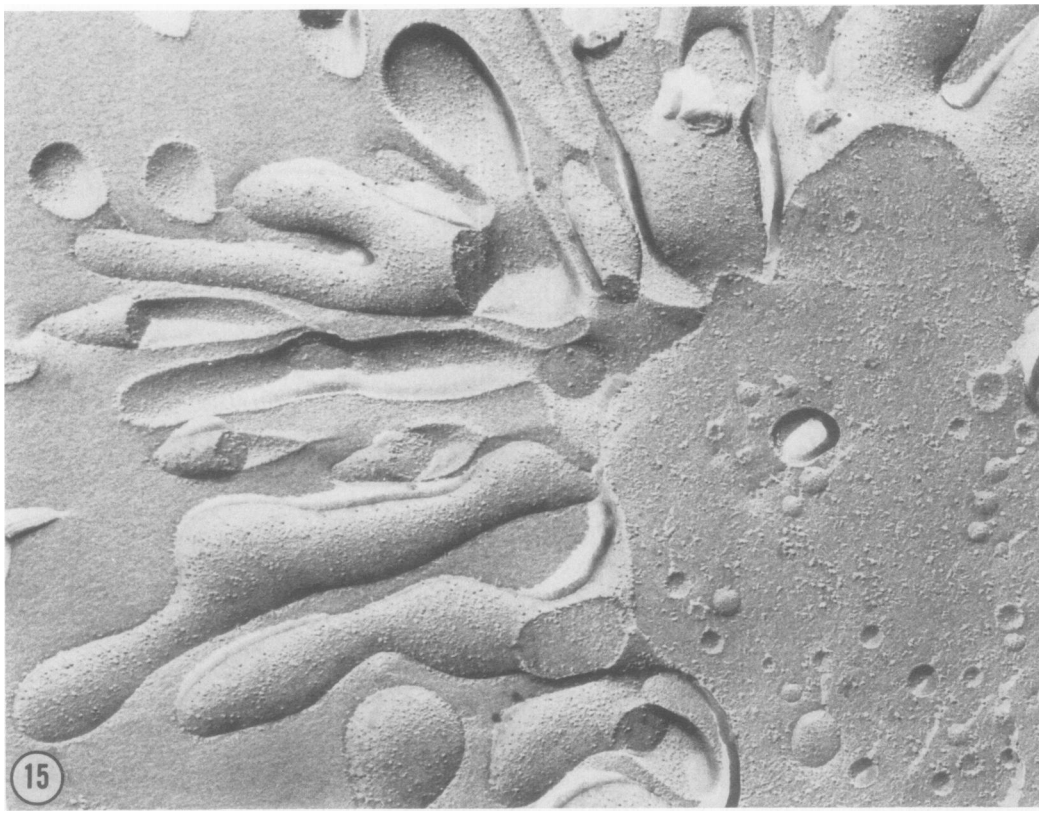

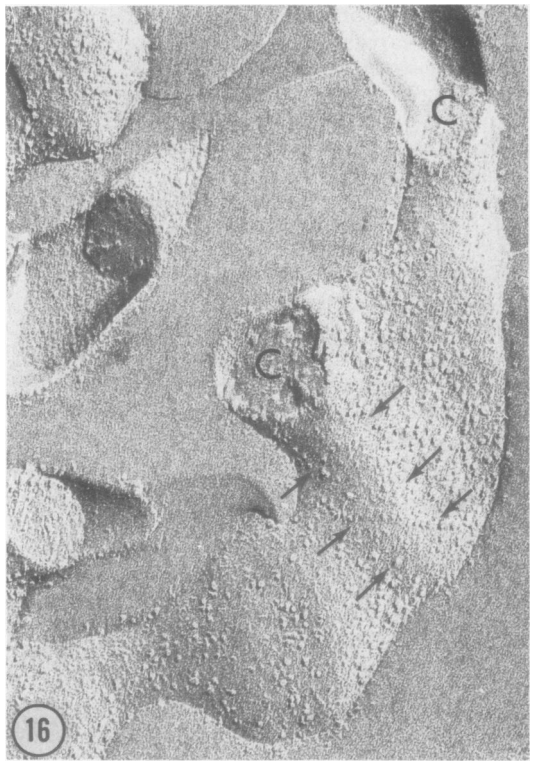

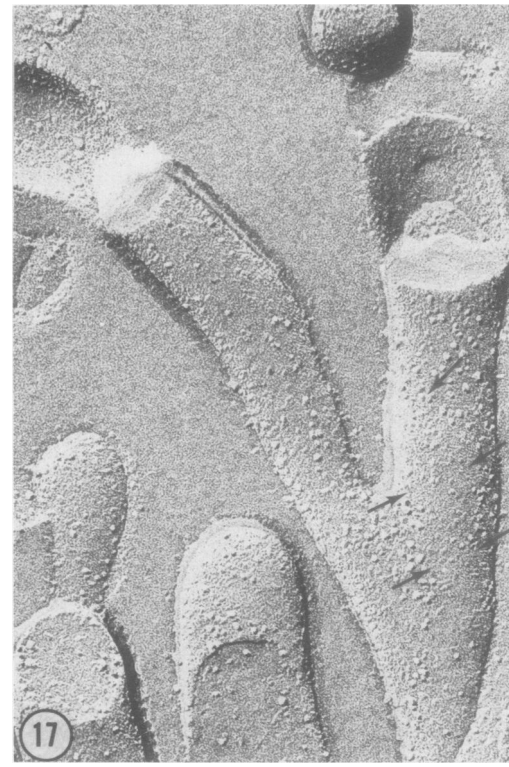

FIG. 15. *Freeze-fracture replica of carrier cells bearing elongated processes similar to the ones shown in thin sections (Fig. 3). As seen in thin sections, some are branched and vary in diameter along their length. Characteristic structural details of elongated processes are shown below.* ×53,000.

distribution of these processes, differentiate them from normal microvilli. Since each of these processes contains one or two hairpin-shaped nucleocapsids contacting the plasmalemma at the ridges, they are considered to be a form of viral bud, hereafter referred to as "hairpin buds." Hairpin buds differ from the viral buds on productive cells by their elongated shape (32) as well as by the fact that the ridges with the underlying nucleocapsids remain separated by narrow strips of membrane resembling that on the rest of the cell surface.

How hairpin buds form is not clear. The attached nucleocapsids might bend the membrane around them to form a hairpin bud or the hairpin nucleocapsids might migrate into and attach to preexisting processes. Since no detached hairpin buds are found, even in serial thin sections, and no other morphological evidence has been found that hairpin buds pinch off from the carrier cell, the hairpin buds appear to be incapable of detaching from the cell. This could be a sufficient explanation for the small amount of infectious virus found in the supernatant of carrier cells.

Straight ridges and hairpin buds are not found in Vero cells acutely infected with the SSPE Mantooth strain or in human prostate cells acutely infected with the SSPE Halle strain, so that these structural alterations do not seem to be characteristic of the virus strain or of the cell type used but, rather, of the persistent state of infection. During the establishment of the chronic infection, carrier cells might have been selected on the basis of their viability. For instance, some host cell factors might induce a change in the flexibility of the nucleocapsids. Indeed, a rigid appearance of the purified nucleocapsid from four different pseudomyxoviruses, including measles, has been described after trypsin treatment of productively infected cells (28, 29, 38). It was proposed that the trypsin triggered an enzyme inside the cells that might cleave certain nucleocapsid proteins, resulting in rigid nucleocapsids. The carrier cells in the present study may be examples of the spontaneous occurrence of a rigid nucleocapsid in situ. However, only the nucleocapsids interacting with the membrane display these characteristics, possibly because the enzyme responsible for protein cleavage is present or active only at the cell membrane.

Since the shape of the nucleocapsids can be inferred from the shape of surface ridges, a possible interpretation of the striking straight course of hairpin nucleocapsids, except where they are bent on themselves at the apices of the hairpin, is that aligned nucleocapsids in carrier cells are more rigid than those in productive cells. However, it must be considered that other changes in the viral components or in the host cell could be responsible for the straight appearance of the nucleocapsid contacting the membrane and the formation of hairpin buds in the carrier cells. The organization and distribution of the attachment sites may be modified, the nucleocapsid coiling preparatory to viral bud formation might be inhibited, or an unusual fluidity of the cell membrane might prevent the pulling together of the nucleocapsids and ridges to exclude intervening host membrane from the viral bud (9). For any of these reasons, normal viral buds might not complete their maturation in carrier cells.

The defective buds, after they have been artificially detached from the cell, appear to contain the complete genomic information necessary for replication since they are able to produce numerous plaques. In this respect, they differ from defective interfering particles of measles (14). However, some of the plaques may also have been produced by normal round buds, which are seen occasionally on the surface of carrier cells, or by other structures not detected by our techniques. The longer length of the carrier cell nucleocapsids, which usually is a multiple of the length of nucleocapsids in productive cells, suggests that repetition of genomic fragments might occur in the hairpin structures.

A typical feature of carrier cells is the polar distribution of ridges and buds, regardless of their structure. It is possible that viral antigens are incorporated into restricted or selected regions of the infected-cell membrane since a diffuse distribution of antigen is never observed in the carrier cells. This postulated distribution of viral antigens differs from that after capping in measles-infected cells which can be induced by antibody and implies movement of viral antigen within the plane of the membrane (23). The peculiar polar distribution of surface antigens might be related to the decreased capacity for cell fusion in carrier cells.

FIG. 16 and 17. *Inner half of the freeze-fractured membrane of elongated processes in carrier cells. Ridges on these processes (delimited by arrows), like those on the rest of the cell membrane (Fig. 13), are characterized by their paucity of intramembrane particles which sometimes form small groups between the ridges. Figure 16 shows two elongated processes that have been cross-fractured (C) close to their origin, and a ridge is seen at each attachment to the cell. Arrows delimit one ridge, but two others are seen on each side of the labeled ones. In Fig. 17, ridges run along both branches of a process, but only the ridge on the right branch is marked with arrows. Intramembrane particles are clustered at the branching point.* ×120,000.

Thus, in carrier cells a defect in incorporation of viral proteins into the cell surface might coexist with a defect in nucleocapsid structure or membrane mobility, and either defect might have a variable expression from cell to cell and from one passage to another. Molecular analysis of nucleocapsid RNA and protein from carrier cells should help clarify the causes of these defects. As yet, there is no evidence that the kind of defective bud formation described here occurs in any disease, including SSPE. Further studies, using similar techniques, on SSPE primary brain cultures from humans (8) or animals (10, 19) should be done to explore whether similar defects in viral maturation can occur spontaneously.

ACKNOWLEDGMENTS

We would like to thank John L. Sever for helpful advice. The excellent technical help of Kathy Worthington and Otto Gutenson is greatly appreciated.

LITERATURE CITED

1. **Anderson, T. F.** 1951. Techniques for the preservation of three dimensional structure in preparing specimens for the electron microscope. Trans. N.Y. Acad. Sci. **13**:130-134.
2. **Birdwell, C. R., E. G. Strauss, and J. H. Strauss.** 1973. Replication of Sindbis virus. III. An electron microscopic study of virus maturation using the surface replica technique. Virology **56**:429-438.
3. **Burnstein, T., L. B. Jacobsen, W. Zeman, and T. T. Chen.** 1974. Persistent infection of BSC-1 cells by defective measles virus derived from subacute sclerosing panencephalitis. Infect. Immun. **10**:1378-1382.
4. **Cooper, P. D.** 1967. The plaque assay of animal viruses, p. 243-311. *In* K. Maramorosch and H. Koprowski (ed.), Methods in virology, vol. 3. Academic Press Inc., New York.
5. **Doi, Y., T. Sanpe, M. Nakajima, S. Okawa, T. Katoh, H. Itoh, T. Sato, K. Oguchi, T. Kumanishi, and T. Tsubaki.** 1972. Properties of a cytopathic agent isolated from a patient with subacute sclerosing panencephalitis in Japan. Jpn. J. Med. Sci. Biol. **25**:321-333.
6. **Dubois-Dalcq, M., and L. H. Barbosa.** 1973. Immunoperoxidase stain of measles antigen in tissue culture. J. Virol. **12**:909-918.
7. **Dubois-Dalcq, M., L. H. Barbosa, R. Hamilton, and J. L. Sever.** 1974. Comparison between productive and latent subacute sclerosing panencephalitis viral infection in vitro. An electron microscopic and immunoperoxidase study. Lab. Invest. **30**:241-250.
8. **Dubois-Dalcq, M., J. M. Coblentz, and A. B. Pleet.** 1974. Subacute sclerosing panencephalitis. Arch. Neurol. **31**:355-363.
9. **Dubois-Dalcq, M., and T. S. Reese.** 1975. Structural changes in the membrane of vero cells infected with a paramyxovirus. J. Cell Biol. **67**:551-565.
10. **Dubois-Dalcq, M., K. Worthington, O. Gutenson, and L. H. Barbosa.** 1975. Immunoperoxidase labeling of subacute sclerosing panencephalitis virus in hamster acute encephalitis. Lab. Invest. **32**:518-526.
11. **Ehrnst, A., L. Weiner, and E. Norrby.** 1974. Fluctuations and distribution of measles virus antigens in chronically infected cells. Nature (London) **248**:691-693.
12. **Gibson, P. E., and T. M. Bell.** 1972. Persistent infection of measles virus in mouse brain cell cultures infected in vivo. Arch. Gesamte Virusforsch. **37**:45-53.
13. **Hall, W. W., and S. J. Martin.** 1973. Purification and characterization of measles virus. J. Gen. Virol. **19**:175-188.
14. **Hall, W. W., and S. J. Martin.** 1974. Defective interfering particles produced during the replication of measles virus. Med. Microbiol. Immunol. **160**:155-164.
15. **Hamilton, R., L. Barbosa, and M. Dubois-Dalcq.** 1973. Subacute sclerosing panencephalitis measles virus: study of biological markers. J. Virol. **12**:632-642.
16. **Haspel, M. V., P. R. Knight, R. G. Duff, and F. Rapp.** 1973. Activation of latent measles virus infection in hamster cells. J. Virol. **12**:690-695.
17. **Horta-Barbosa, L., D. A. Fuccillo, J. L. Sever, and W. Zeman.** 1969. Subacute sclerosing panencephalitis isolation of measles virus from a brain biopsy. Nature (London) **221**:974.
18. **Iwasaki, Y., H. Koprowski, D. Muller, V. ter Meulen, and Y. M. Kackell.** 1973. Morphogenesis and structure of a virus in cells cultured from brain tissue from two cases of multiple sclerosis. Lab. Invest. **28**:494-500.
19. **Johnson, K. P., and E. Norrby.** 1974. Subacute sclerosing panencephalitis (SSPE) agent in hamsters. III. Induction of defective measles infection in hamster brain. Exp. Mol. Pathol. **21**:166-178.
20. **Klein, G., P. Clifford, E. Klein, R. T. Smith, J. Minowada, F. M. Kouriosky, and J. H. Burchenal.** 1967. Membrane immunofluorescence reactions of Burkitt lymphoma cells from biopsy specimens and tissue cultures. J. Natl. Cancer Inst. **39**:1027-1044.
21. **Knight, P., R. Duff, R. Glaser, and F. Rapp.** 1973. Characteristics of the release of measles virus from latently infected cells after co-cultivation with BSC-1 cells. Intervirology **2**:287-298.
22. **Knight, P., R. Duff, and F. Rapp.** 1972. Latency of human measles virus in hamster cells. J. Virol. **10**:995-1001.
23. **Lampert, P. W., B. S. Joseph, and M. Oldstone.** 1975. Antibody-induced capping of measles virus antigens on plasma membrane studied by electron microscopy. J. Virol. **15**:1248-1255.
24. **Lennette, E. H., and N. J. Schmidt. (ed.).** 1969. Diagnostic procedure for viral and rickettsial infections, 4th ed. American Public Health Association, Inc., New York.
25. **Menna, J. H., A. R. Collins, and T. D. Flanagan.** 1975. Characterization of an in vitro persistent-state measles virus infection: establishment and virological characterization of the BGM/MV cell line. Infect. Immun. **11**:152-158.
26. **Minagawa, T.** 1971. Studies on the persistent infection with measles virus in HeLa cells. I. Clonal analysis of cells of carrier cultures. Jpn. J. Microbiol. **15**:325-331.
27. **Minagawa, T.** 1971. Studies on the persistent infection with measles virus in HeLa cells. II. The properties of carried virus. Jpn. J. Microbiol. **15**:333-340.
28. **Mountcastle, W. E., R. W. Compans, L. A. Caliguiri, and P. W. Choppin.** 1970. Nucleocapsid protein subunits of simian virus 5, Newcastle disease virus, and Sendai virus. J. Virol. **6**:677-684.
29. **Mountcastle, W. E., R. W. Compans, H. Lackland, and P. W. Choppin.** 1974. Proteolytic cleavage of subunits of the nucleocapsids of the paramyxovirus simian virus 5. J. Virol. **14**:1253-1261.
30. **Norrby, E.** 1967. A carrier cell line of measles virus in Lu 106 cells. Arch. Gesamte Virusforsch. **20**:215-224.
31. **Norrby, E. C. J., and P. Magnusson.** 1965. Some morphological characteristics of the internal component of measles virus. Arch. Gesamte Virusforsch. **17**:443-447.
32. **Orenstein, J. M., and I. B. Weinstein.** 1973. Filamen-

tous forms of enveloped A particles in cell cultures from chemically induced rat hepatomas. Cancer Res. 33:1998–2004.

33. **Raine, C. S., L. A. Feldman, R. D. Sheppard, L. H. Barbosa, and M. B. Bornstein.** 1974. Subacute sclerosing panencephalitis virus. Observations on a neuroadapted strain and non neuroadapted strain in organotypic central nervous system cultures. Lab. Invest. 31:42–53.
34. **Raine, C. S., L. A. Feldman, R. D. Sheppard, and M. B. Bornstein.** 1973. Subacute sclerosing panencephalitis virus in cultures of organized central nervous tissue. Lab. Invest. 28:627–640.
35. **Rustigian, R.** 1966. Persistent infection of cells in culture by measles virus. I. Development and characteristics of HeLa sublines persistently infected with complete virus. J. Bacteriol. 92:1792–1804.
36. **Rustigian, R.** 1966. Persistent infection of cells in culture by measles virus. II. Effect of measles antibody on persistently infected HeLa sublines and recovery of a HeLa clonal line persistently infected with incomplete virus. J. Bacteriol. 92:1805–1811.
37. **Steele, R. W., D. A. Fuccillo, S. A. Hensen, M. M. Vincent, and J. A. Bellanti.** 1976. Specific inhibitory factors of cellular immunity in children with Subacute Sclerosing panencephalitis. J. Pediatr. 88:56–62.
38. **Waters, D. J., and R. H. Bussell.** 1974. Isolation and comparative study of the nucleocapsids of measles and canine distemper viruses from infected cells. Virology 61:64–79.
39. **Waters, D. J., R. T. Hersh, and R. H. Bussell.** 1972. Isolation and characterization of measles nucleocapsid from infected cells. Virology 48:278–281.